Mathematics

AIMS Mathematics, 11(5): 13384–13411.
DOI: 10.3934/math.2026552
Received: 23 January 2026
Revised: 19 April 2026
Accepted: 27 April 2026
Published: 14 May 2026

https://www.aimspress.com/journal/Math

Research article

A lower ranked set sampling framework for enhanced stress-strength reliability assessment with exponentiated Pareto-distributed data

Amal S. Hassan [1],Mohamed A. Abd Elgawad[2], Majdah Mohammed Badr[3] and Rokaya Elmorsy Mohamed [4,*]

[1] Faculty of Graduate Studies for Statistical Research, Cairo University, 5 Dr. Ahmed Zewail Street, Giza, 12613, Egypt
[2] Department of Mathematics and Statistics, College of Science, Imam Mohammad Ibn Saud Islamic University (IMSIU), Riyadh, 11432, Saudi Arabia
[3] Department of Mathematics and Statistics, College of Science, University of Jeddah, Jeddah, Saudi Arabia
[4] Department of Mathematics, Statistics and Insurance, Faculty of Management Sciences, Sadat Academy for Management Sciences, Cairo, 11728, Egypt

* **Correspondence:** Email: rokayaelmorsy@gmail.com.

Abstract: Real-world constraints like time and sample size limitations often restrict access to complete data. Consequently, it is beneficial to study estimation problems based on information from existing data. In these circumstances, employing a suitable sampling strategy to obtain more effective estimators is crucial. In this study, we addressed the estimation of the stress-strength reliability parameter ζ based on lower record ranked set sampling. The stress and strength variables adhere to the exponentiated Pareto distribution with a common second shape parameter. The maximum likelihood and Bayesian estimation methods are suggested for estimating ζ. The Bayesian estimator is provided in the case of gamma and uniform priors using different loss functions. Two distinct parametric bootstrap techniques are established, and Bayesian credible intervals are generated with the help of the Markov chain Monte Carlo method. A comprehensive Monte Carlo simulation study was developed to evaluate the precision of different estimators. A simulation study highlighted that the Bayesian estimates, which are calculated under different loss functions, perform more effectively than a comparable maximum likelihood estimates. It was discovered that the percentile

bootstrap method produced better estimates than the normal-bootstrap method, with shorter average lengths and higher coverage probability. Two datasets from physical scientific applications further support the effectiveness and usefulness of the methodology.

Keywords: exponentiated Pareto distribution; Bayesian estimation; weighted squared error loss function; bootstrapping; Metropolis-Hastings sampler
Mathematics Subject Classification: 62F10, 62C10

1. Introduction

1.1. Overview of record values

In many real-world applications, record values and the inferences drawn from them are crucial, such as in life testing, sports, medicine, and hydrology. The successive extremes in the series of random variables are known as record values (RVs). Chandler [1] first proposed the idea of RVs, which are the successive extremes in a sequence of random variables. Records that show an upward trend are called upper records, and those that show a downward trend are called lower records. Foster and Stuart [2] added to the field by investigating hypothesis tests for establishing the distribution of RVs based on the sums and differences of upper and lower RVs within a series.

1.2. Ranked set sampling and its extensions

Ranked set sampling (RSS) was initially proposed by McIntyre [3] for situations in which the variables being studied are easy to rank but challenging to measure directly. By significantly increasing the amount of information in the sample, this sampling technique improves the efficiency of population statistical analysis. When estimating the population mean, Takahasi and Wakimoto [4] showed that the sample mean under RSS is a better estimator than simple random sampling. For other studies, refer to [5–7].

One major limitation of traditional record-based sampling is that it frequently produces little data. To overcome this constraint, Salehi and Ahmadi [8] extended the conventional RSS method with a new sampling technique called record RSS (RRSS), which improves data efficiency. The RRSS, specifically, the lower RRSS (LRRSS), is used in this article for its practical applicability in minimizing experimental expenses and enhancing sampling effectiveness.

1.3. The LRRSS scheme

The LRRSS methodology works as follows: Suppose m_1 independent random sequences in which the k-th sampling sequence is completed whenever the k-th record is observed. The final record value in each sequence is the only observation that can be used for analysis. The observations that are available are $\boldsymbol{D} = (D_{1,1}, D_{2,2}, ..., D_{m_1,m_1})^T$ if we indicate the final record for the k-th sequence in this plan by $D_{k,k}$. A record-ranked set sample of size m_1 is then denoted by $\boldsymbol{D}$. This process of observation can be explained by the following

$$\begin{array}{cccccc} 1 & D_{(1),1} & & & \to D_{1,1} = & D_{(1),1} \\ 2 & D_{(1),1} & D_{(2),1} & & \to D_{2,2} = & D_{(2),2} \\ \vdots & \vdots & \vdots\ddots & & \vdots & \vdots \\ m_1 & D_{(1),m_1} & D_{(2),m_1} & \cdots\ D_{(m_1),m_1} & \to D_{m_1,m_1} = & D_{m_1,(m_1)} \end{array}$$

in which the k-th ordinary record in the h-th sequence is denoted by $D_{(k),h}$. Therefore, $\boldsymbol{D} = (D_{1,1}, D_{2,2}, ..., D_{m_1,m_1})^T$ is the LRRSS of size m_1. Note that, in contrast to regular records, D_{m_1,m_1} are independent random variables that are not always in that order.

1.4. Procedure for the LRRSS scheme

Step 1: Generate m_1 independent random sequences of observations from the target population.
Step 2: For each sequence, identify lower records (values that are smaller than all previous values in that sequence). The k-th sequence is stopped when its k-th lower record appears. Thus, sequence 1 stops at its 1st record, sequence 2 stops at its 2nd record, and so on until the last sequence m_1, which stops at its m_1-th record.
Step 3: Only the exact record values that meet the stopping criteria are kept for analysis, while all previous observations within the sequence are omitted. The selected values are:

i. From sequence 1: $D_{11} = D_{(1)1}$.
ii. From sequence 2: $D_{22} = D_{(2)2}$.
iii. From sequence m_1: $D_{m_1m_1} = D_{m_1(m_1)}$.

Step 4: Collect these specific records into a vector $\boldsymbol{D} = (D_{1,1}, D_{2,2}, ..., D_{m_1,m_1})^T$.

The LRRSS model is most suitable when smaller values of a degradation or failure-related parameter can be observed, and the process of collecting information is expensive or destructive. This sampling scheme is recommended for the following engineering contexts:

i. Fatigue fracture propagation in aerospace structures: Cyclic loading is applied to a number of similar structures, such as wing spars. Although there are periodic inspections, each structure's smallest crack initiation life is noted since it represents the period of time when the structure is most susceptible to failure. Once the k-th lower record appears, the experiment is over. The LRRSS is made up of all sequences' final record observations. The probability that the applied stress will exceed the residual strength is then calculated using this dataset.
ii. Breaking-down voltage of insulators in high voltage applications: There can be multiple specimens used in testing the voltage, which will gradually increase. The breaking-down voltage is initially recorded to be the lowest figure, but further tests may result in even lower breaking-down voltages owing to wear and tear. It is economically wise to focus on recording such lower figures.

The above examples have been given to show that the LRRSS phenomenon emerges automatically in the context of reliability engineering if only low extremes or very low extremes occur.
Suppose that $g(.,\theta)$ represents the population's probability density function (PDF) and $G(.,\theta)$ its cumulative distribution function (CDF). According to Arnold et al. [9], the joint density of $\boldsymbol{D}$ is then determined using the marginal density of ordinary records.

$$g_{\boldsymbol{D}}(d) = \prod_{k=1}^{m_1} \frac{\left[-\log G(d_{k,k};\theta)\right]^{k-1} g(d_{k,k})}{(k-1)!}, \qquad \theta \in \Theta, \tag{1}$$

where $\boldsymbol{d} = (d_{1,1}, d_{2,2}, ..., d_{m_1,m_1})^T$ is the observed LRRSS of $\boldsymbol{D} = (D_{1,1}, D_{2,2}, ..., D_{m_1,m_1})^T$ and Θ is the parameter space. This scheme was employed by Salehi and Ahmadi [8] to forecast future statistics, such as ordinary record values and order statistics. To estimate the proportional hazard rate model parameter, Salehi et al. [10] contrasted the RRSS scheme with usual records. Information measures for RRSS were obtained by Eskandarzadeh et al. [11]. Moreover, Paul and Thomas [12] suggested concomitant RRSS for circumstances in which measuring the variable of interest is prohibitively expensive or difficult. Safariyan et al. [13] used an RRSS scheme to propose some improved estimators for stress-strength reliability. Sadeghpour et al. [14] looked at estimating the stress strength model (SSM) under the assumption that Q and V follow the generalized exponential distribution based on LRRSS. Further works on SSM were investigated by Dong and Gui [15] for the generalized Rayleigh distribution.

1.5. Literature review on SSM

A major topic in the statistical literature is the analysis of SSM, represented as $\zeta = Pr(Q < V)$, where the stress Q does not exceed the strength V. The SSM was first presented by Birnbaum [16] and has since attracted a lot of attention from reliability statistics researchers. The SSM has many applications in practical engineering, notably in product life testing and material reliability analysis and design. To guarantee aircraft safety, for instance, life tests are necessary for aircraft components in the aerospace industry. During its use, the product will be subject to a range of external stresses, including temperature, humidity, wind, and pressure. Apart from the impact of these external stresses, the product possesses a certain level of resilience to withstand these stresses (see Kotz et al. [17] for more examples). Nowadays, the SSM is widely used in many fields, especially in tackling problems with reliability evaluation. Researchers have examined statistical inferences on SSM by choosing different distributions for stress (Q) and strength (V) distributions, taking into account sampling methodologies. For instance, studies on SSM using complete samples include the estimation of $Pr(Q < V)$ when Q and V follow independent generalized exponential distributions, as discussed by Kundu and Gupta [18] and Raqab et al. [19]. Estimation of SSM in the case of Burr X distribution was suggested by the researchers in [20]. Bayesian and hierarchical Bayesian SSM under partially accelerated life testing was suggested by [21]. The inference of SSM based on progressive censoring from the Chen and logistic exponential distributions was provided by the researchers in [22,23]. The SSM using the inverted exponentiated Rayleigh distribution under block censoring and k-records was discussed by Newer [24]. As shown in the study of Nassr et al. [25], the use of data from progressive hybrid censoring can successfully perform the task of reliability analysis on clinical and medical data. For additional studies of SSM, see [26–28].

Statistical inference of the SSM has been examined by researchers in the context of record data. Baklizi [29] suggested the estimation of SSM in the case of exponential distribution using lower RVs. The estimation of ζ from the proportional hazard rate model and the proportional reversed hazard family was investigated by the researchers in [30, 31], respectively. Estimation of SSM for the Pareto model was suggested by Juvairiyya and Anilkumar [32] using upper RVs. Moreover, estimation of SSM for the proportional reversed hazard family, based on lower RVs, was investigated by Chaturvedi and Malhotra [33]. Estimation of ζ for the Weibull distribution, based on records, was studied by Pak et al. [34]. Yu et al. [35] discussed the estimation of ζ for unit-Burr III distribution using upper RVs. Elkalzah et al. [36] suggested classical and Bayesian estimation of the SSM under the discrete distribution using RVs, with a practical application to a high-voltage capacitor. Hassan et

al. [37] proposed a reliability analysis of the SSM for the inverted exponentiated Pareto distribution based on RVs.

1.6. Motivation and objectives of the study

The exponentiated Pareto distribution (EPD) has been widely employed in this domain since being introduced for use with extreme events by Pickands [38]. This flexibility is attributable to the EPD's failure rates having a bathtub shape that may reduce or invert according to the values of the shape parameters. Consequently, the EPD provides certain benefits in applications with extremes, especially in hydrology and reliability engineering due to the fact that it is more resistant than other distributions to heavy- and light-tail situations compared to the exponential distribution (see Chen and Cheng [39]). The failure rate, although monotonic, is flexible enough to accommodate the monotonic and non-monotonic failure rate functions, which can have decreasing and inverted bathtub shapes, respectively, depending on the value of the shape parameter. The non-monotonic failure rate functions are especially useful in the analysis of survival data when, for example, the mortality rate is high initially, and then the rate decreases over time, as shown by Gupta et al. [40]. The EPD is a mixture of the Pareto and the exponential distributions, which can model the time between failures. Moreover, Aarssen and Haan [41] suggested the use of the EPD in the analysis of the annual maximum wind speed and the maximum floods in the Feather River. Additional uses include the estimation of the finite limit of human longevity [42,43], the simulation of high concentrations in short-range atmospheric dispersion [44], and estimation of SSM with an application to insurance data [45]. Estimations of single and multi-components in SSM based on EPD was suggested by [46–48]. Jabbari Nooghabi [49] looked into how to estimate the EPD when there were outliers. Parameter estimators of the EPD under progressive censored was examined by Mahmoud et al. [50]. Using ranked set sampling, Khamnei et al. [51] investigated the estimation of the EPD parameters.

The two-parameter EPD with shape parameters $\rho, \mu > 0,$ has the following PDF and CDF, respectively:

$$g(v) = \mu\rho(1+v)^{-\rho-1}\left[1-(1+v)^{-\rho}\right]^{\mu-1}; \qquad \rho,\mu,v > 0, \tag{2}$$

and,

$$G(v) = \left[1-(1+v)^{-\rho}\right]^{\mu}; \qquad \rho,\mu,v > 0. \tag{3}$$

To the best of our knowledge, only one study [14] has examined the estimation of the SSM with the help of the LRRSS approach. The application of the LRRSS approach is effective in reducing the cost associated with experiments compared to the traditional approach of random sampling and standard lower RVs. This is the motivation behind our attempt to estimate the SSM for the EPD. The motivation for the use of EPD stems from remarkable adaptability in simulating failure rate behaviors, such as decreasing and inverted bathtub shapes. Because of its versatility, the EPD can be used to model a variety of real-world datasets in reliability analysis. In this work, we present the classical and Bayesian estimation of the SSM with the help of the LRRSS approach, where the variables are jointly independent with an EPD. This work can be summarized as follows:

- The maximum likelihood estimate (MLE) of ζ along with the Bayesian estimate (BE) using gamma (informative) and uniform (non-informative) priors are discussed.
- The BE under the squared error loss function (SELF), weighted SELF (WSELF), and minimum

expected loss function (MLF) are obtained.

- Create Bayesian credible intervals (BCIs) and the highest posterior density (HPD) intervals using the Markov Chain Monte Carlo (MCMC) algorithm. Two parametric bootstrap methods, namely percentile bootstrap confidence intervals (Boot-p-CIs) and bootstrap t confidence intervals (Boot-t- CIs), are established.
- Extensive Monte Carlo simulation research is created to assess the accuracy of estimators. The methodology's application to two real datasets taken from a physical scientific field further supports its applicability and efficacy.

This document is structured in the following manner: The MLE of SSM is obtained in Section 2. Boot-p-CIs and Boot-t-CIs of ζ are generated in Section 3. Bayes estimator of ζ is discussed in Section 4. The performance of the proposed point and interval estimates is analyzed and compared in Section 5 through a simulation analysis. In Section 6, we analyze real data sets on the engineering challenges, and in the final section, we offer closing thoughts.

2. Maximum likelihood estimation

In this section, we give the expression of ζ with its MLE. To obtain the formula for $\zeta = Pr(Q < V)$, we assume that the strength (V) has the EPD (ρ, μ_1), and the stress (Q) has the EPD (ρ, μ_2), where the stress Q and V are assumed to be independent random variables. Then, the formula of ζ is provided as follows:

$$\zeta = P(Q < V) = \int_0^\infty G_Q(v) g_V(v) dv, \tag{4}$$

where $g_V(v)$ is the PDF of the strength random variable (V) and $G_Q(v)$ is the CDF of the stress random variable (Q) at v. Using the PDF (2) and CDF (3), Eq (4) becomes:

$$\begin{aligned} \zeta &= P(Q < V) = \int_0^\infty G_Q(v) g_V(v) dv \\ &= \int_0^\infty \mu_1 \rho (1+v)^{-\rho-1} \left[1-(1+v)^{-\rho}\right]^{\mu_1+\mu_2-1} dv = \frac{\mu_1}{\mu_1+\mu_2}. \end{aligned} \tag{5}$$

As seen in Eq (5), the SSM depends on parameters μ_1 and μ_2. It is interesting to note that under the assumption of a common shape parameter ρ, the closed-form expression for ζ in Eq (5) provides a similar shape to the independent exponential SSM (see, e.g., Kotz et al. [17]). This follows from the specific integration of the EPD's PDF and CDF under the common shape ρ assumption. However, unlike the scale parameters of the exponential distribution, μ_1 and μ_2 act as shape parameters here, and the parent EPD offers more flexible hazard rates (including inverted bathtub shapes) than the constant hazard rate of the exponential distribution. This common value of ρ simplifies the subsequent estimation problem and is the basis for the inference under the LRRSS scheme.

Figure 1 shows the SSM's 3D graphs with different parameter values. It can be seen that the value of ζ decreases as both parameters (μ_1 and μ_2) increase. The slope becomes steeper with higher values of parameters, indicating faster reliability decline. The color gradient highlights this change, with blue representing lower reliability values and red representing higher reliability values.

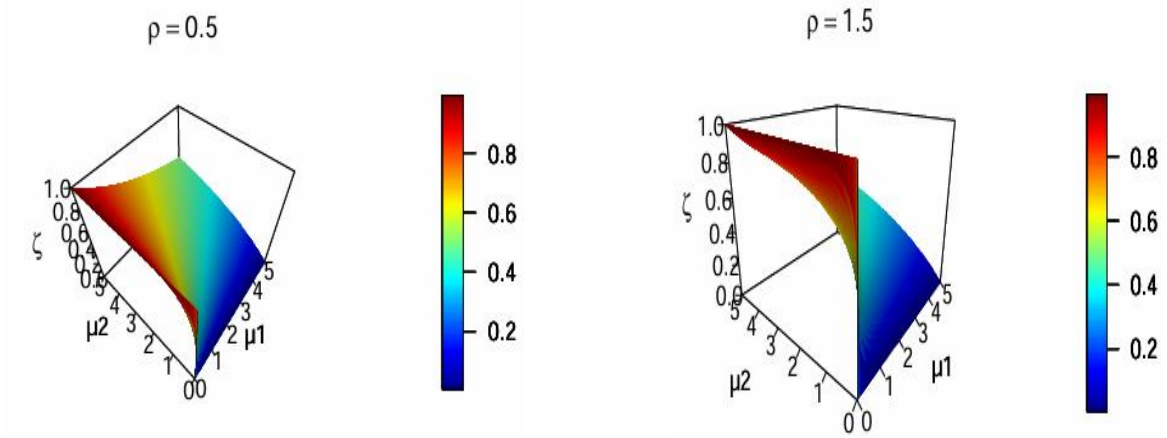

Figure 1. The 3D plots of ζ for the selected values of parameters.

To get the MLE of ζ, suppose that $\boldsymbol{d} = (d_{1,1}, d_{2,2}, ..., d_{m_1,m_1})^T$ is the observed LRRSS of $\boldsymbol{D} = (D_{1,1}, D_{2,2}, ..., D_{m_1,m_1})^T$ from the strength (V), while $\boldsymbol{c} = (c_{1,1}, c_{2,2}, ..., c_{m_2,m_2})^T$ is the observed LRRSS of $\boldsymbol{C} = (C_{1,1}, C_{2,2}, ..., C_{m_2,m_2})^T$ from stress (Q). Based on PDF (2) and CDF (3), suppose that $V \sim (\rho, \mu_1)$, and $Q \sim (\rho, \mu_2)$ and then, according to Equation (1), the likelihood function of independent Q and V is given by:

$$L(\Im \mid \underline{\boldsymbol{d}}, \underline{\boldsymbol{c}}) = \prod_{k=1}^{m_1} \frac{\left[-\log\left[1-\left(1+v_{k,k}\right)^{-\rho}\right]^{\mu_1}\right]^{k-1}}{(k-1)!} \mu_1 \rho \left(1+v_{k,k}\right)^{-\rho-1} \left[1-\left(1+v_{k,k}\right)^{-\rho}\right]^{\mu_1-1} \times \prod_{l=1}^{m_2} \frac{\left[-\log\left[1-\left(1+q_{l,l}\right)^{-\rho}\right]^{\mu_2}\right]^{l-1}}{(l-1)!} \mu_2 \rho \left(1+q_{l,l}\right)^{-\rho-1} \left[1-\left(1+q_{l,l}\right)^{-\rho}\right]^{\mu_2-1}, \tag{6}$$

where, $\Im \equiv (\mu_1, \mu_2, \rho)$ is the set of parameters. The log-likelihood function of (6), represented as $\ln L^*$ is given by:

$$\begin{aligned} \ln L^* \propto\ & m_1 \log \mu_1 + m_2 \log \mu_2 - (\rho+1)\left[\sum_{k=1}^{m_1} \log\left(1+v_{k,k}\right) + \sum_{l=1}^{m_2} \log\left(1+q_{l,l}\right)\right] \\ & + (m_1+m_2)\log\rho + \sum_{k=1}^{m_1} (k-1)\log(-\mu_1 H_k(v_{k,k}, \rho)) + (\mu_1 - 1)\sum_{k=1}^{m_1} \log H_k(v_{k,k}, \rho) \\ & + \sum_{l=1}^{m_2} (l-1)\log(-\mu_2 S_l(q_{l,l}, \rho)) + (\mu_2 - 1)\sum_{k=1}^{m_1} \log S_l(q_{l,l}, \rho), \end{aligned}$$

where $H_k(v_{k,k}, \rho) = \log\left[1-\left(1+v_{k,k}\right)^{-\rho}\right]$ and $S_l(q_{l,l}, \rho) = \log\left[1-\left(1+q_{l,l}\right)^{-\rho}\right]$.

Thus, the following is a formulation of the normal equations:

$$\frac{\partial \ln L^*}{\partial \mu_1} = \frac{m_1}{\mu_1} + \frac{m_1^2 - m_1}{2\mu_1} + \sum_{k=1}^{m_1} H_k(v_{k,k}, \rho) = 0, \tag{7}$$

$$\frac{\partial \ln L^*}{\partial \mu_2} = \frac{m_2}{\mu_2} + \frac{m_2^2 - m_2}{2\mu_2} + \sum_{l=1}^{m_2} S_l(q_{l,l}, \rho) = 0, \tag{8}$$

and

$$\begin{aligned} \frac{\partial \ln L^*}{\partial \rho} = \frac{m_1 + m_2}{\rho} - \left[\sum_{k=1}^{m_1} \log\left(1+v_{k,k}\right) + \sum_{l=1}^{m_2} \log\left(1+q_{l,l}\right) \right] + \sum_{k=1}^{m_1} \frac{(\mu_2 - 1) S_l'(q_{l,l})}{S_l(q_{l,l})} \\ - \sum_{k=1}^{m_1} \frac{(k-1) H_k'(v_{k,k})}{\mu_1 H_k(v_{k,k})} + \sum_{k=1}^{m_1} \frac{(\mu_1 - 1) H_k'(v_{k,k})}{H_k(v_{k,k})} - \sum_{l=1}^{m_2} \frac{(l-1) S_l'(q_{l,l})}{\mu_2 S_l(q_{l,l})} = 0. \end{aligned} \tag{9}$$

Here, $H_k'(v_{k,k}, \rho) = \dfrac{\partial H_k(v_{k,k}, \rho)}{\partial \rho} = \dfrac{\log\left(1+v_{k,k}\right)}{\left(1+v_{k,k}\right)^{\rho} - 1}$, $S_l'(q_{l,l}, \rho) = \dfrac{\partial S_l(q_{l,l}, \rho)}{\partial \rho} = \dfrac{\log\left(1+q_{l,l}\right)}{\left(1+q_{l,l}\right)^{\rho} - 1}$.

From Eqs (7) and (8), the MLEs $\hat{\mu}_{1(MLE)}$ and $\hat{\mu}_{2(MLE)}$ of parameters μ_1 and μ_2 are obtained as a function of parameter ρ, using optimization techniques such as the Newton-Raphson algorithm, as follows:

$$\hat{\mu}_{1(MLE)} = \frac{-(m_1^2 + m_1)}{2\sum_{k=1}^{m_1} H_k(v_{k,k}, \rho)}, \quad \hat{\mu}_{2(MLE)} = \frac{-(m_2^2 + m_2)}{2\sum_{l=1}^{m_2} S_l(q_{l,l}, \rho)}. \tag{10}$$

By substituting $\hat{\mu}_{1(MLE)}$ and $\hat{\mu}_{2(MLE)}$ in Eq (10) into Eq (9), the MLE $\hat{\rho}_{(MLE)}$ of ρ is produced by numerically solving the resulting non-linear equation. Using expression (5) and the MLE's invariance characteristic, we obtain the MLE for ζ, represented as $\hat{\zeta}_{(MLE)}$.

3. Parametric bootstrap confidence intervals

The bootstrapping methods described in the seminal study by Tibshirani and Efron [52] are used in this research to determine CIs for parameter ζ. Particularly, we use two bootstrapping techniques, boot-p and boot-t, which are methods for calculating CIs in statistical models. The boot-p approach, also known as the percentile method, is a non-parametric method in which the empirical percentiles of the bootstrapped statistic are directly computed to determine the CI. Although boot-p is a simple and popular technique for creating CIs, it might not be the best choice in circumstances with small sample sizes or highly skewed data distributions. The outline of the procedure for obtaining the boot-p and boot-t CIs is as follows:

Algorithm 1: Boot-p method

1. Initially, based on the independent observed LRRSS as we explained in subsection (1.4), we employ the given data sets $\underline{\boldsymbol{D}}$ and $\underline{\boldsymbol{C}}$, to solve the likelihood equations and determine the MLEs of the parameters $\hat{\mu}_{1(MLE)}, \hat{\mu}_{2(MLE)}$, and $\hat{\rho}_{(MLE)}$.
2. Next, for a fixed value of m_1, we generate a bootstrap LRRSS of size m_1, denoted as $\underline{\boldsymbol{d}}^* = (d_{1,1}^*, d_{2,2}^*, ..., d_{m_1,m_1}^*)^T$ from EPD$(\hat{\mu}_{1(MLE)}, \hat{\rho}_{(MLE)})$. Similarly, for a fixed value of m_2, we generate LRRSS of size m_2, denoted as $\underline{\boldsymbol{c}}^* = (c_{1,1}^*, c_{2,2}^*, ..., c_{m_2,m_2}^*)^T$ from EPD$(\hat{\mu}_{2(MLE)}, \hat{\rho}_{(MLE)})$.
3. Based on the generated samples, we calculate the bootstrap estimates of $\hat{\Im}^*_{(MLE)} \equiv (\hat{\mu}^*_{1(MLE)}, \hat{\mu}^*_{2(MLE)}, \hat{\rho}^*_{(MLE)})$, and $\hat{\zeta}^*_{(MLE)}$.
4. Steps 2 and 3 are repeated for a sufficiently large number of times, denoted as B, to obtain a set of ordered values of $\hat{\zeta}^*_{(MLE)}$, denoted as $\hat{\zeta}^*_{(MLE)}(1) \le \hat{\zeta}^*_{(MLE)}(2) \le ... \le \hat{\zeta}^*_{(MLE)}(B)$.
5. Let $\hat{\zeta}^{boot-p}_{(MLE)} = H_1^{-1}(Z)$ for a given z, where $H_1(Z) = P(\hat{\zeta}^*_{(MLE)} \le z)$ be the CDF of $\hat{\zeta}^*_{(MLE)}$.
6. Last, the $100(1-\tau)\%$ approximate boot-p CI for ζ is acquired as

$$\left[\hat{\zeta}^{boot-p}_{(MLE)}\left(\frac{\tau}{2}\right), \hat{\zeta}^{boot-p}_{(MLE)}\left(1-\tau/2\right)\right].$$

The boot-t procedure is a modification of the traditional t-interval and is intended for use when the sample size is constrained or when data may not meet traditional normality assumptions. The data are resampled by replacement to generate multiple samples called bootstrap samples. These samples are employed to compute a statistic analogous to a traditional t-statistic. The following is a summary of the steps involved in creating the boot-t CI:

Algorithm 2: Boot-t method

Repeat steps 1 through 4 of the previously described boot-p procedure in Algorithm 1.

7. For every $\hat{\zeta}^*_{(MLE)}$, calculate $T^* = \dfrac{\left(\hat{\zeta}^*_{(MLE)} - \hat{\zeta}_{(MLE)}\right)}{\sqrt{\text{var}(\hat{\zeta}^*_{(MLE)})}}$, to obtain ordered values $T_1^* \le T_2^* \le ... \le T_B^*$.
8. Let $\hat{\zeta}^{boot-t}_{(MLE)} = \hat{\zeta}_{(MLE)} + H^{-1}(Z)\sqrt{\text{var}(\hat{\zeta}^*_{(MLE)})}$, where $H^{-1}(Z)$ is the CDF of T^* for a given z.
9. Then $100(1-\tau)\%$ approximate boot-t CI is

$$\left[\hat{\zeta}^{boot-t}_{(MLE)}\left(\frac{\tau}{2}\right), \hat{\zeta}^{boot-t}_{(MLE)}\left(1-\tau/2\right)\right].$$

4. Bayesian estimation

In this section, we investigate the Bayesian estimation of unknown parameters and the SSM ζ. In many lifespan models, the gamma distribution is an often-used informative prior (IP) for parameters due to its ease of use and computational effectiveness. Its structure, which includes a tail that extends to infinity and a peak close to zero, makes it easier to derive the posterior distribution. As a result, assume that the prior distributions of μ_1, μ_2, and ρ follow independent gamma priors. Hence, the following mathematical expression of the joint prior density function

$$\pi(\zeta) \propto \mu_1^{\alpha_1 - 1} \mu_2^{\alpha_2 - 1} \rho^{\alpha_3 - 1} e^{-(\beta_1 \mu_1 + \beta_2 \mu_2 + \beta_3 \rho)}; \ \alpha_i, \beta_i > 0, i = 1,2,3. \tag{11}$$

Here, the values of $\alpha_i, \beta_i > 0, i = 1,2,3$ are chosen to reflect earlier interpretations of μ_1, μ_2, and ρ

where their selected values are discussed in sub-section (4.2). Note that IP becomes non-IP (NIP) when values of $\alpha_1, \alpha_2, \alpha_3, \beta_1, \beta_2, \beta_3$ are selected to approach zero. Using Eqs (6) and (11), the joint posterior density of $\mu_1, \mu_2,$ and ρ is obtained as follows:

$$\Pi(\Im \mid \underline{\boldsymbol{d}}, \underline{\boldsymbol{c}}) \propto \mu_1^{m_1+\alpha_1-1} \mu_2^{m_2+\alpha_2-1} \rho^{m_1+m_2+\alpha_3-1} \exp\left\{\sum_{k=1}^{m_1}(k-1)\log\left[-\mu_1 H_k(v_{k,k},\rho)\right] + \sum_{l=1}^{m_2}(l-1)\log\left[-\mu_2 S_l(q_{l,l},\rho)\right]\right\}$$
$$\times \exp\left\{(\mu_1-1)\sum_{k=1}^{m_1}\log\, H_k(v_{k,k},\rho) + (\mu_2-1)\sum_{k=1}^{m_1}\log\, S_l(q_{l,l},\rho)\right\}$$
$$\times \exp\left\{-\rho\left[\beta_3 + \sum_{l=1}^{m_2}\ln\left(1+q_{l,l}\right) + \sum_{k=1}^{m_1}\ln\left(1+v_{k,k}\right)\right] - \mu_1\beta_1 - \mu_2\beta\right\}.$$

The marginal posterior densities of $\mu_1, \mu_2,$ and ρ are:

$$\Pi_1(\mu_1 \mid \rho, \underline{\boldsymbol{d}}, \underline{\boldsymbol{c}}) \propto \mu_1^{m_1+\alpha_1-1} \exp\left\{-\mu_1\beta_1 + \sum_{k=1}^{m_1}(k-1)\log\left[-\mu_1 H_k(v_{k,k},\rho)\right] + \mu_1\sum_{k=1}^{m_1}\log\, H_k(v_{k,k},\rho)\right\}, \tag{12}$$

$$\Pi_2(\mu_2 \mid \rho, \underline{\boldsymbol{d}}, \underline{\boldsymbol{c}}) \propto \mu_2^{m_2+\alpha_2-1} \exp\left\{-\mu_2\beta_2 + \sum_{l=1}^{m_2}(l-1)\log\left[-\mu_2 S_l(q_{l,l},\rho)\right] + \mu_2\sum_{k=1}^{m_1}\log\, S_l(q_{l,l},\rho)\right\}, \tag{13}$$

and,

$$\Pi_3(\rho \mid \mu_1, \mu_2, \underline{\boldsymbol{d}}, \underline{\boldsymbol{c}}) \propto \rho^{m_1+m_2+\alpha_3-1} \exp\left\{\sum_{k=1}^{m_1}(k-1)\log\left[-\mu_1 H_k(v_{k,k},\rho)\right] + \sum_{l=1}^{m_2}(l-1)\log\left[-\mu_2 S_l(q_{l,l},\rho)\right]\right\}$$
$$\times \exp\left\{(\mu_1-1)\sum_{k=1}^{m_1}\log\, H_k(v_{k,k},\rho) + (\mu_2-1)\sum_{k=1}^{m_1}\log\, S_l(q_{l,l},\rho)\right\} \tag{14}$$
$$\times \exp\left\{-\rho\left[\beta_3 + \sum_{l=1}^{m_2}\ln\left(1+q_{l,l}\right) + \sum_{k=1}^{m_1}\ln\left(1+v_{k,k}\right)\right]\right\}.$$

However, our analysis does not enable the closed-form computation of the posterior distributions of $\mu_1, \mu_2,$ and $\rho,$ given in Eqs (12)–(14). In addition, we will compute the lower and upper limits of the BCIs and HPD intervals of unknown parameters. Therefore, we employ the Metropolis-Hastings (M-H) sampler with normal proposal distribution to solve it numerically. The BEs of $\mu_1, \mu_2,$ and ρ can be computed by following the same procedure as above if the values of the hyper-parameters are adjusted to values close to zero; in this instance, the prior is an NIP.

4.1. The MCMC method

In the MCMC approach, the BEs are produced using the M-H sampler. To calculate their HPD credible intervals, the BEs use the MCMC under the SELF, WSELF, and MLF. The MCMC simulation approach is used to assess the performance of many estimates derived from Bayes computation. The Bayesian paradigm generates diverse posterior samples with varying sample size values using MCMC sampling algorithms. Important subclasses of MCMC algorithms include the M-H with normal proposal distribution. An overview of the M-H sampler is provided below:

Algorithm 3: M-H method

1. Initialize the values $\left(\mu_1^{(0)}, \mu_2^{(0)}, \rho^{(0)}\right)$.

2. Next, for a fixed value of m_1, we generate a LRRSS of size m_1, denoted as $\boldsymbol{d} = (d_{1,1}, d_{2,2}, ..., d_{m_1,m_1})^T$ from $\text{EPD}(\mu_1, \rho)$. Similarly, for a fixed value of m_2, we generate LRRSS of size m_2, denoted as $\boldsymbol{c} = (c_{1,1}, c_{2,2}, ..., c_{m_2,m_2})^T$ from $\text{EPD}(\mu_2, \rho)$.

3. Set $w = 1$.

4. Generate $\mu_1^{(w)}, \mu_2^{(w)}$, and $\rho^{(w)}$ from normal proposal distributions $N(\mu_1^{(w-1)}, V_{\mu_1})$, $N(\mu_2^{(w-1)}, V_{\mu_2})$, and $N(\rho^{(w-1)}, V_{\rho})$, respectively:

- Draw μ_1^* from the normal proposal distribution $N(\mu_1^{(w-1)}, V_{\mu_1})$, μ_2^* from the normal proposal distribution $N(\mu_2^{(w-1)}, V_{\mu_2})$, and ρ^* from the normal proposal distribution $N(\rho^{(w-1)}, V_{\rho})$.
- Compute the acceptance probability

$$\phi_{\mu_1}\left(\mu_1^{(w-1)}, \mu_1^*\right) = \min\left[1, \frac{\Pi_1^*(\mu_1^* \left| \mu_2^{(w-1)}, \rho^{(w-1)}, data\right.)}{\Pi_1^*(\mu_1^{(w-1)} \left| \mu_2^{(w-1)}, \rho^{(w-1)}, data\right.)}\right],$$

$$\phi_{\mu_2}\left(\mu_2^{(w-1)}, \mu_2^*\right) = \min\left[1, \frac{\Pi_2^*(\mu_2^* \left| \mu_1^{(w-1)}, \rho^{(w-1)}, data\right.)}{\Pi_2^*(\mu_2^{(w-1)} \left| \mu_1^{(w-1)}, \rho^{(w-1)}, data\right.)}\right],$$

$$\phi_{\rho}\left(\rho^{(w-1)}, \rho^*\right) = \min\left[1, \frac{\Pi_3^*(\rho^* \left| \mu_1^{(w-1)}, \mu_2^{(w-1)}, data\right.)}{\Pi_3^*(\rho^{(w-1)} \left| \mu_1^{(w-1)}, \mu_2^{(w-1)}, data\right.)}\right].$$

- Generate u_1, u_2, and u_3 from $U(0,1)$.
- Confirm the proposal and place

$\mu_1^{(w)} = \mu_1^*$. If $u_1 \le \phi_{\mu_1}\left(\mu_1^{(w-1)}, \mu_1^*\right)$. Elsewhere, deny the proposal and place $\mu_1^{(w)} = \mu_1^{(w-1)}$,

$\mu_2^{(w)} = \mu_2^*$. If $u_2 \le \phi_{\mu_2}\left(\mu_2^{(w-1)}, \mu_2^*\right)$. Elsewhere, deny the proposal and place $\mu_2^{(w)} = \mu_2^{(w-1)}$,

$\rho^{(w)} = \rho^*$. If $u_3 \le \phi_{\rho}\left(\rho^{(w-1)}, \rho^*\right)$. Elsewhere, deny the proposal and place $\rho^{(w)} = \rho^{(w-1)}$.

5. Compute $\mu_1^{(w)}, \mu_2^{(w)}, \rho^{(w)}$, and $\zeta^{(w)}$.

6. Set $w = w + 1$.

7. Repeat Steps 4–6, N times.

Now, the Bayes estimate $\tilde{\zeta}_{(BE)}$, of parameter ζ under the SELF, WSELF, and MLF are obtained, respectively, as

$$\tilde{\zeta}_{SELF} = \frac{1}{N-M}\sum_{w=M+1}^{N} \tilde{\zeta}_{(BE)}^{(w)},\ \tilde{\zeta}_{WSELF} = \left[\frac{1}{N-M}\sum_{w=M+1}^{N}\left(\tilde{\zeta}_{(BE)}^{(w)}\right)^{-1}\right]^{-1},\ \text{and}\ \tilde{\zeta}_{MLF} = \frac{\left(\frac{1}{N-M}\sum_{w=M+1}^{N}\left(\tilde{\zeta}_{(BE)}^{(w)}\right)^{-1}\right)}{\left(\frac{1}{N-M}\sum_{w=M+1}^{N}\left(\tilde{\zeta}_{(BE)}^{(w)}\right)^{-2}\right)},$$

where, N is a total iteration of simulation and M represents the burn-in period. To obtain the $100(1-\tau)\%$ BCI of ζ, the MCMC samples are first sorted in ascending order as follows: $\left(\zeta^{[M+1]} < \zeta^{[2]} < ... < \zeta^{[N]}\right)$. Next, obtain the following $100(1-\tau)\%$ BCI bounds:

$\left(\zeta^{[\tau(N-M)/2]}, \zeta^{[(1-\tau/2)(N-M)]}\right)$. Finally, we determine the HPD of ζ, as $\left(\zeta^{[b^*]}, \zeta^{[b^*+(1-\tau)(N-M)]}\right)$, where $b^* = M+1,...,N$ is specified as $b^* = \arg\min_{1\le b\le \tau(N-M)} \left\{\zeta^{[b+[(1-\tau)(N-M)]]} - \zeta^{[b]}\right\}$.

4.2. Elicitation of Hyper-parameters

It is noteworthy to mention that the hyper-parameters of the IPs are estimated using the MLEs from the available data. This is because the prior distribution is informed using the available data, and this is referred to as the empirical Bayes procedure. This is different from the fully Bayesian procedure, where the hyper-parameters are assumed to be known independently of the available data.

In this study, the determination of hyper-parameters depends on IPs, derived from the MLEs for $\text{EPD}(\mu_1, \mu_2, \rho)$. This is accomplished by lining up the variance and mean of $(\hat{\mu}^j_{1(MLE)}, \hat{\mu}^j_{2(MLE)}, \hat{\rho}^j_{(MLE)})$ with the corresponding parameters of gamma priors. Here, $j = 1,2,...,i$, and i denotes the number of available samples from the $\text{EPD}(\mu_1, \mu_2, \rho)$ (Dey et al. [53] and Singh and Tripathi [54]). Equating the mean and variance estimates of gamma priors with the mean and variance of $\hat{\Im}^j_{(MLE)}$, we obtain the following equations:

$$\frac{\alpha_j}{\beta_j} = \frac{1}{i}\sum_{j=1}^{i} \hat{\Im}^j_{(MLE)}, \quad \frac{\alpha_j}{\beta_j^2} = \frac{1}{i-1}\sum_{j=1}^{i}\left(\hat{\Im}^j_{(MLE)} - \frac{1}{i-1}\sum_{j=1}^{i}\hat{\Im}^j_{(MLE)}\right)^2.$$

By solving the mentioned pair of equations, we can express the estimated hyper-parameters as follows:

$$\alpha_j = \frac{\left(\frac{1}{i}\sum_{j=1}^{i}\hat{\Im}^j_{(MLE)}\right)^2}{\frac{1}{i-1}\sum_{j=1}^{i}\left(\hat{\Im}^j_{(MLE)} - i^{-1}\sum_{j=1}^{i}\hat{\Im}^j_{(MLE)}\right)^2}, \text{ and } \beta_j = \frac{\frac{1}{i}\sum_{j=1}^{i}\hat{\Im}^j_{(MLE)}}{\frac{1}{i-1}\sum_{j=1}^{i}\left(\hat{\Im}^j_{(MLE)} - i^{-1}\sum_{j=1}^{i}\hat{\Im}^j_{(MLE)}\right)^2}.$$

5. Numerical illustration

For our comprehensive simulation study, we assess estimation methods in SSM analysis, with a particular emphasis on EPD and LRRSS. We use a variety of strategies and several performance metrics, such as absolute biases (ABs), mean squared errors (MSEs), and coverage probability (CP), to evaluate the effectiveness of different estimation methods. The estimators' accuracy is evaluated using ABs and MSEs, which reveal how well they captured the true values of the parameters. Moreover, the CP provides a gauge of the approaches' dependability by acting as an indicator of their robustness and CI coverage. To conduct our evaluation, we calculate the ABs and MSEs of MLE and BE under different loss functions, considering different sample sizes and varying values of the parameters. Additionally, we create a variety of CI types, such as boot-p and boot-t CIs, BCIs, and HPD credible intervals. The average interval lengths (AILs) of these intervals and the associated CP are evaluated. For each analysis, the 95% estimated boot-p and boot-t CIs are obtained after computing the MLEs. Additionally, we conduct 1000 replications to guarantee the validity of our results.

The EPD is used to generate two independent LRRSS for the V and the Q variables in each simulation. Both variables have a common shape parameter, ρ. In particular, random observations are taken from the parent EPD for every record sequence. The sequence ends when the k-th lower record appears, and the last record value is held. The LRRSS are obtained by repeating this across m_1 and m_2 separate sequences as: $\boldsymbol{D} = (D_{1,1}, D_{2,2}, ..., D_{m_1,m_1})^T$ and $\boldsymbol{C} = (C_{1,1}, C_{2,2}, ..., C_{m_2,m_2})^T$, respectively. For calculations, we utilize R 4.4.2 program, a statistical programming language. To examine the performance of the suggested estimators under the LRRSS scheme, a comprehensive Monte Carlo simulation analysis is conducted as three sets of the true parameters and the associated real value of ζ, where the common parameter $\rho = 2$; these sets are as displayed in:

$$\begin{array}{llll} Set\ 1: & \mu_1 = 0.5 & \mu_2 = 1.5 & \rho = 2 \quad \zeta = 0.25 \\ Set\ 2: & \mu_1 = 0.5 & \mu_2 = 0.5 & \rho = 2 \quad \zeta = 0.50 \\ Set\ 3: & \mu_1 = 3.8 & \mu_2 = 0.2 & \rho = 2 \quad \zeta = 0.95 \end{array}$$

where, Set 1: Represents a low reliability case, and, hence, has high variability, Set 2: Represents a moderate case or balanced parameters, and Set 3: Represents a high reliability case, and, hence, lower probability of failure. With these three sets of parameter settings, we can capture reliability regimes:

- Stable systems (low probability of failure).
- Highly variable systems (heavy tail behavior).

Additionally, we examine nine sample sizes, including (m_1, m_2) = (3, 3), (3, 5), (3, 7), (5, 3), (5, 5), (5, 7), (7, 3), (7, 5), and (7, 7). These configurations illustrate the small to moderate sample sizes that are common in record-based sampling systems. LRRSS, unlike conventional random sampling, generates fewer observations because it relies on lower record values. Unequal sample sizes ($m_1 \neq m_2$) represent real-world scenarios where stress and strength variables may have different amounts of information available.

The identifiability of the parameters is maintained with respect to the LRRSS technique since the lower record values contain enough information about the true distribution. The joint distribution of the record values depends exclusively on the two shape parameters such that the same distribution cannot be produced using any other set of parameter values. This ensures that the identifiability of the parameters is maintained even after record sampling. As far as the interpretation of the parameters is concerned, it remains the same with respect to the LRRSS technique, i.e., the shape parameters specify the tail and hazard features.

In the Bayesian framework study, hyper-parameter values are selected as described in Section 4.2 for IP and set to a value that is close to zero; in this instance, the prior is an NIP. We conduct 10,000 iterations using the MCMC technique, discarding the first 2,000 values as burn-in to reduce reliance on the initial state. In the MCMC technique, the BEs are produced using an M-H sampler, enabling us to compute 95% BCIs and HPDs.

Tables A.1 and A.2 and Figures 2−9 display the outcomes of the simulation. Taking into account the outcomes of the simulation, the following conclusions can be drawn:

- The ABs and MSEs for MLEs and BEs of ζ tend to reduce as the number of records (m_1, m_2) rises (see Table A.1 and Figures 2−4). This demonstrates the consistency and efficiency of the proposed procedures under the LRRSS system.
- The performance of BEs of ζ derived from loss functions like SELF, WSELF, and MLF is superior to that of MLEs, as the MLEs typically have larger ABs and MSEs than BEs (see Table A.1).
- It is noticeable that, in every scenario, the MSEs and ABs of ζ estimates for IPs have the lowest values compared to the other NIPs (see Table A.1 and Figures 3, 4, and 9).

- The improvement is more significant for cases where both samples increase simultaneously, as captured by $m_1 = m_2$.
- The MLE of ζ is more variable, especially for small samples. This variability is expected due to the limited information in the LRRSS data.
- The BEs of ζ listed under MLF typically outperform those listed under SELF and WSELF. However, when compared to other BEs, those under SELF had the worst (see Table A.1 and Figures 3, 4, and 9).
- The IP and the MLF of ζ estimates regularly produce statistically better results:
  a) The IP successfully integrates previous knowledge into the posterior analysis, as it is built from a gamma distribution whose hyper-parameters are based on reliable estimates. Given the nature of the LRRSS scheme, which produces less data points than a comparable SRS despite its efficiency, this method serves to stabilize the estimate process, which is very important. The IP estimate of ζ achieves the lowest MSEs and ABs across all scenarios by effectively minimizing the posterior standard deviation by narrowing the posterior distribution around a reasonable parameter area.
  b) The features of the EPD and the resulting posterior distribution of the reliability ζ are primarily responsible for the MLF estimator's better performance when compared to other loss functions. The posterior distribution is most likely skewed, according to diagnostic plots. The MLF effectively reduces the genuine posterior expected risk since the SELF generates the posterior mean, which is not resilient to skewness. The MLF offers a more accurate and precise point estimate by producing an estimate that is closer to the posterior mode or median in skewed distributions. This results in consistently lower MSEs and superior CPs for the derived HPD credible intervals.
- Additionally, it should be mentioned that BCIs perform better than boot-p and boot-t intervals for both IPs and NIPs of ζ.
- From Table A.2, the CP of ζ for boot-p is superior to boot-t. The boot-p often has lower AIL than boot-t. Additionally, the length of BCIs reduces as record numbers rise (see Figure 6).
- Based on AIL and CP, the HPD credible intervals of ζ in IPs perform better than those in NIPs in every scenario (see Figures 5 and 7 and Table A.2).
- It appears that the MSE of MLEs and BEs of ζ reaches their maximum at $\zeta = 0.50,$ while at the increased values of ζ, specifically 0.95, the MSE is relatively small (see Figures 8 and 9).
- At high reliability levels, variations between estimators become less significant. In contrast, at moderate reliability levels, Bayesian estimators provide more reliable inference, emphasizing their benefit when uncertainty is highest.
- Finally, the MCMC diagnostics plots are shown in Figure 10 to verify that the IP and the NIP estimate of ζ have satisfactory mixing and convergence, although the IP continuously performs better than the NIP in terms of:
  1) More rapid convergence (trace and cumulative plots).
  2) Reduced posterior uncertainty (histograms that are narrower).
  3) Reduced autocorrelation due to more effective sampling.

Therefore, when prior knowledge is relevant and appropriately described, the IP-based Bayesian estimation yields more accurate and stable estimates of reliability parameter ζ, which is consistent with theoretical expectations.

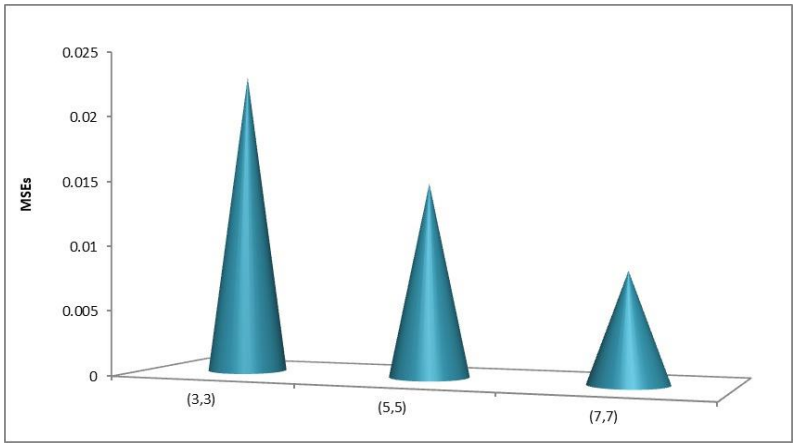

Figure 2. The MSEs of $\hat{\zeta}_{(MLE)}$ for different record numbers at $\zeta = 0.50$.

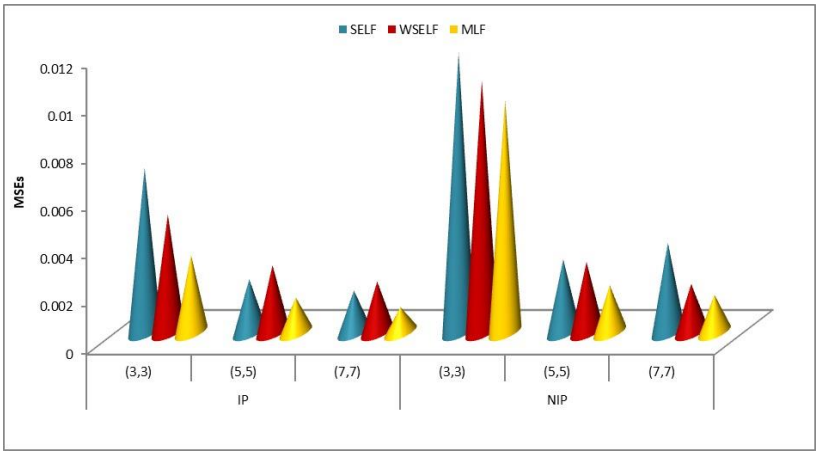

Figure 3. The MSEs of $\tilde{\zeta}_{(BE)}$ in case of IP and NIP for different record numbers at $\zeta = 0.25$.

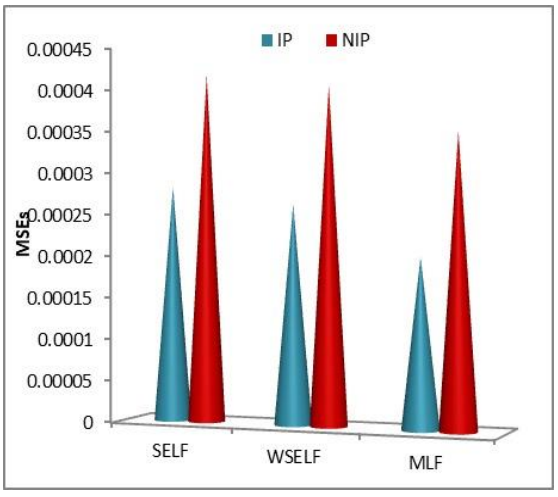

Figure 4. The MSEs of $\tilde{\zeta}_{(BE)}$ for all loss functions at record numbers (m_1, m_2)=(5,5) at $\zeta = 0.95$.

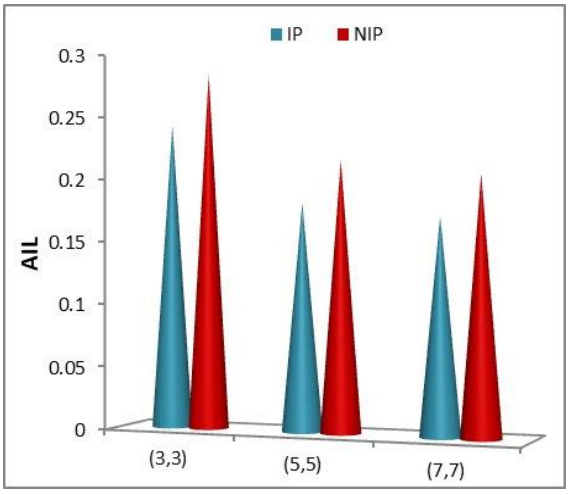

Figure 5. The AILs of IP and NIP estimates for different record numbers (m_1, m_2) at $\zeta = 0.50$.

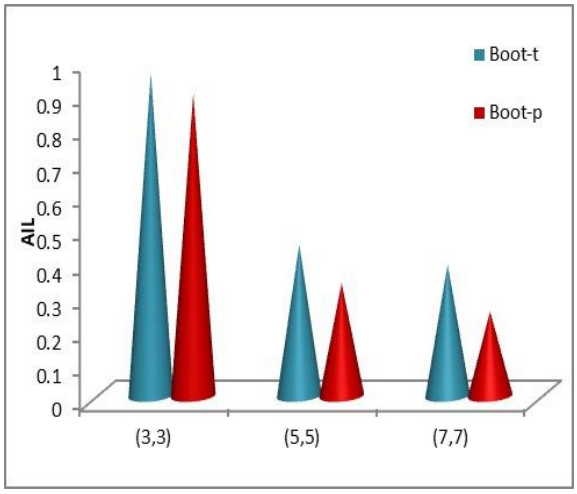

Figure 6. The AIL of boot-t and boot-p for different record numbers of (m_1, m_2) at $\zeta = 0.25$.

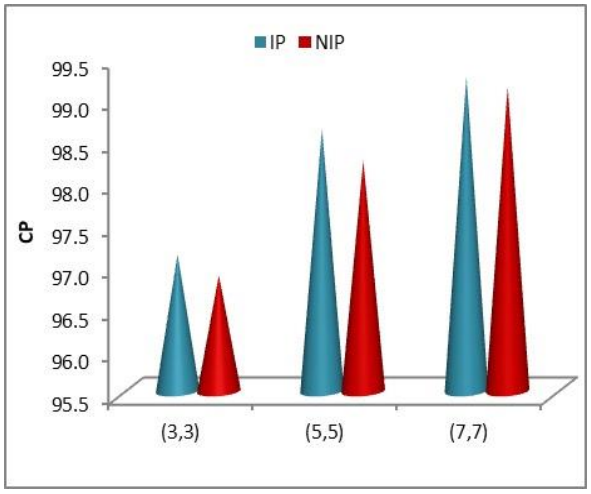

Figure 7. The CP of IP and NIP estimates for different record numbers of (m_1, m_2) at $\zeta = 0.95$.

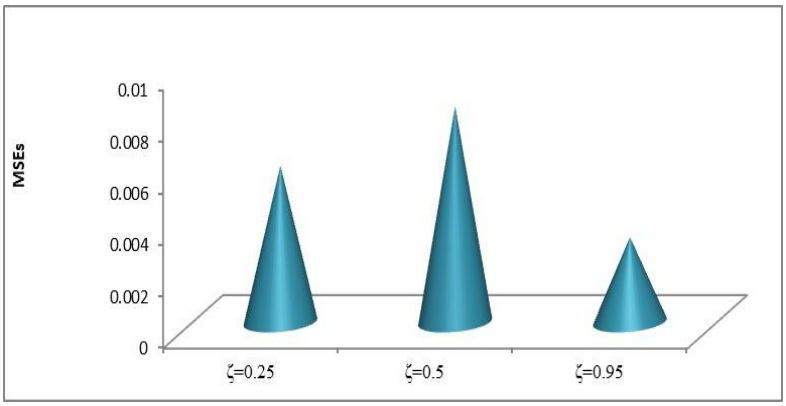

Figure 8. The MSE of $\hat{\zeta}_{MLE}$ for different true values of ζ at (m_1, m_2) = (7, 7).

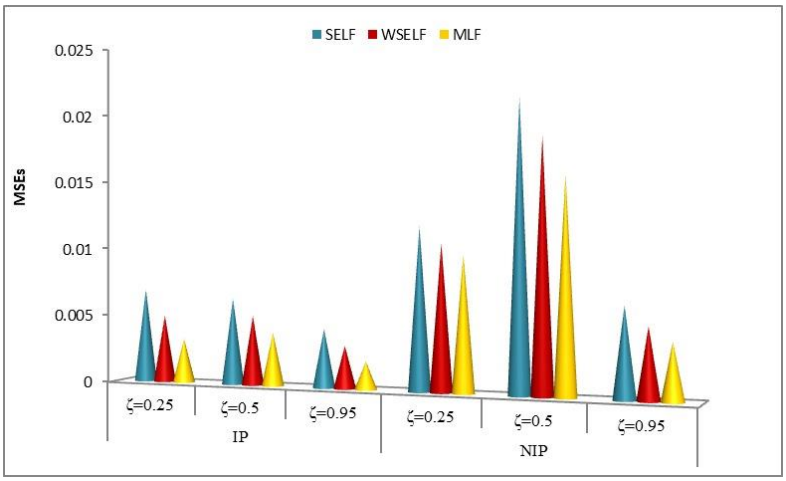

Figure 9. The MSE of $\tilde{\zeta}_{(BE)}$ in case of IP and NIP for different true values of ζ at (m_1, m_2) = (3, 3).

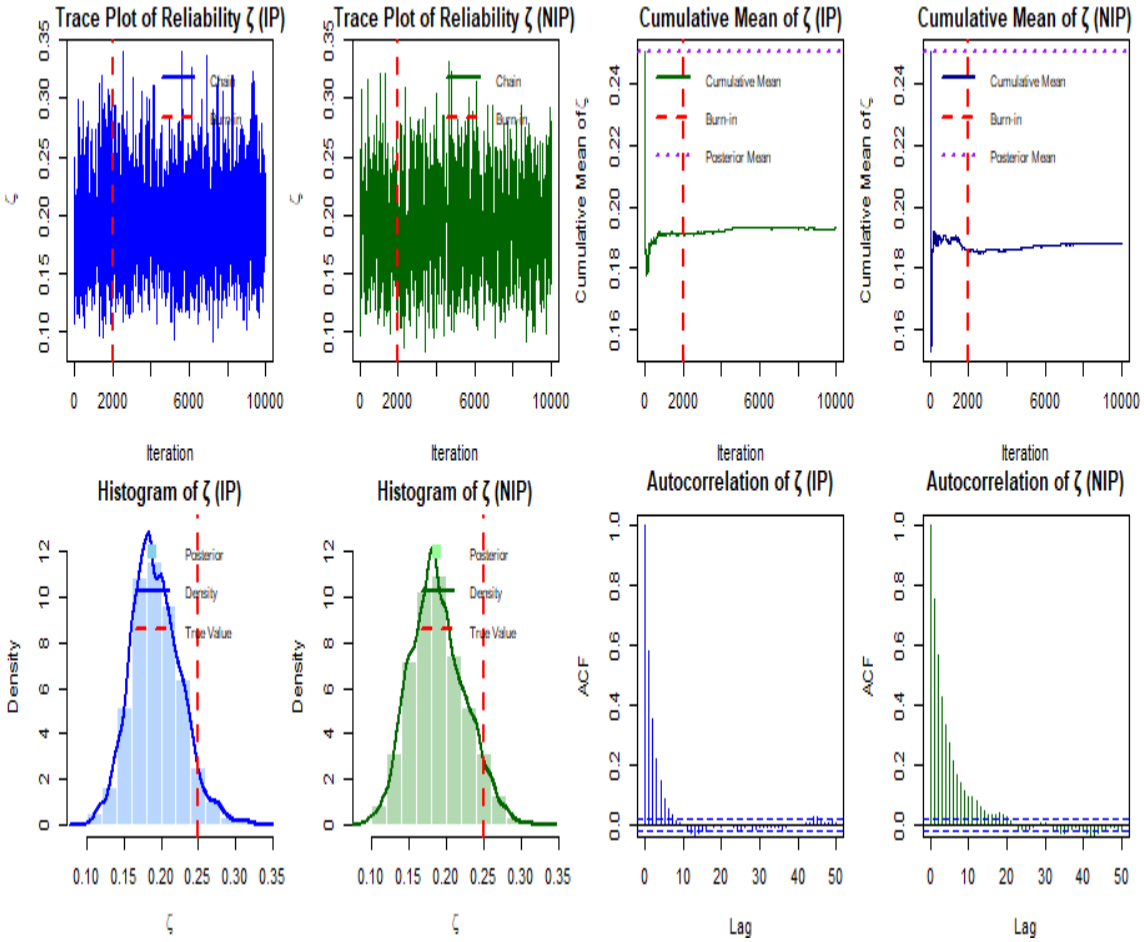

Figure 10. The MCMC plots of ζ estimate at $(m_1, m_2) = (3,5)$ for Set 1.

Figure 10 offers strong empirical evidence regarding the identifiability of the model parameters under the LRRSS model framework. The different shapes of the graphs, which correspond to set 1 of parameter values, demonstrate that the changes in the parameter values (especially the shape parameter values) cause significant differences in the performance of the reliability measure estimation. This is due to the property of the model, which states that the distribution of lower record values is a function only of the unique model parameters. Hence, the results depicted in Figure 10 provide empirical evidence that the model parameters are identifiable. This finding is further supported by posterior diagnostics, where trace plots for all parameters reveal rapid mixing and stationarity across chains with no evidence of divergent transitions or multimodality, hence validating sample reliability and parameter identifiability.

6. Data analysis

To demonstrate the results obtained in the preceding section, we intend to provide the analysis of two real datasets. In a life test experiment, electrical insulating fluids developed for transformers are subjected to constant-voltage stress. The failure or breakdown of each specimen is measured in minutes. Nelson [55] supplied data of seven groups of specimens evaluated at voltages between 26 and 38 kilovolts (kV) for lifetime modeling using the inverse power-law model. Lawless [56] also

provided these datasets. The first dataset (V) represents the 32 kV, where the system's resistance is under relatively moderate conditions, and the second dataset (Q) represents the 36 kV, as higher voltage levels impose more severe operating conditions and accelerate failure. For self-containment, Datasets (I) and (II) show the failure times in 180 minutes for groups of specimens exposed to 32 kV and 36 kV.

Dataset (I): V = (0.4, 82.85, 9.88, 89.29, 215.10, 2.75, 0.79, 15.93, 3.91, 0.27, 0.69, 100.58, 27.80, 13.95, 53.24).

Dataset (II): Q = (1.97, 0.59, 2.58, 1.69, 2.71, 25.50, 0.35, 0.99, 3.99, 3.67, 2.07, 0.96, 5.35, 2.90, 13.77).

The first step is to ascertain whether the EPD is suitable for the analysis of the specified datasets. The MLEs and associated standard errors (SEs) are computed based on each dataset sample. Among the goodness-of-fit criteria evaluated are the following: Akaike information criterion (AIC), Bayesian information criterion (BIC), corrected AIC (CAIC), Hannan-Quinn information criterion (HQIC), Kolmogorov-Smirnov (K-S) test statistic and its corresponding P-value, Anderson-Darling (A*) test statistic, and Cramer-von Mises (W*) test statistic. These criteria are used to assess the suitability of the EPD compared to other distributions, such as the generalized Rayleigh distribution (GRD), the inverse Weibull distribution (IWD), and the Burr XII distribution (BXIID). This demonstrates that the EPD has the highest p-value and the lowest values for other statistics; as a result, the EPD is the best option among the others and fits the two real datasets well. The MLE of model parameters along with their SEs are shown in Table 1, and Table 2 provides the goodness-of-fit statistics for both datasets. Additionally, Figures 11 and 12 indicate that the EPD is an appropriate model to fit to both datasets.

Table 1. MLEs with their SEs of the two real datasets.

Data	Model	$\hat{\mu}$	$SE(\hat{\mu})$	$\hat{\rho}$	$SE(\hat{\rho})$
I	EPD	1.4869	0.1072	0.4892	0.2210
	GRD	0.8814	0.2787	0.2629	0.0007
	IWD	0.9557	0.0471	0.7132	0.0609
	BXIID	1.1919	0.0974	0.3305	0.1685
II	EPD	3.7100	0.1128	1.4931	0.2552
	GRD	0.2877	0.0828	0.0059	0.0029
	IWD	1.4812	0.1034	1.0275	0.1478
	BXIID	2.4588	0.0995	0.3767	0.1566

Table 2. Model adequacy and goodness of fit test statistics for the two real datasets.

Data	Model	AIC	BIC	CAIC	HQIC	A*	W*	K-S	P-value
I	EPD	138.931	140.346	144.347	138.916	0.607	0.099	0.175	0.688
	GRD	701.667	703.083	707.083	701.651	10.2579	1.8016	0.651	0.000
	IWD	139.723	140.718	144.719	139.687	0.639	0.107	0.197	0.535
	BXIID	139.885	141.301	145.301	139.870	0.660	0.119	0.203	0.505
II	EPD	75.470	76.886	80.886	75.454	0.210	0.034	0.116	0.974
	GRD	84.331	85.747	89.747	84.316	1.451	0.299	0.301	0.106
	IWD	76.278	77.694	81.694	76.263	0.312	0.056	0.155	0.813
	BXIID	76.474	77.890	81.890	76.458	0.335	0.069	0.172	0.704

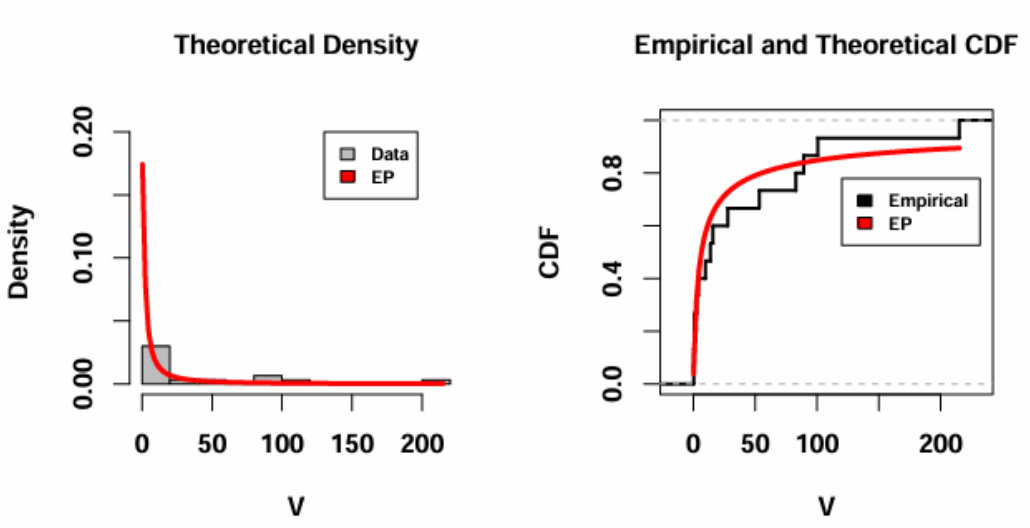

Figure 11. Estimated PDF and CDF for the first dataset.

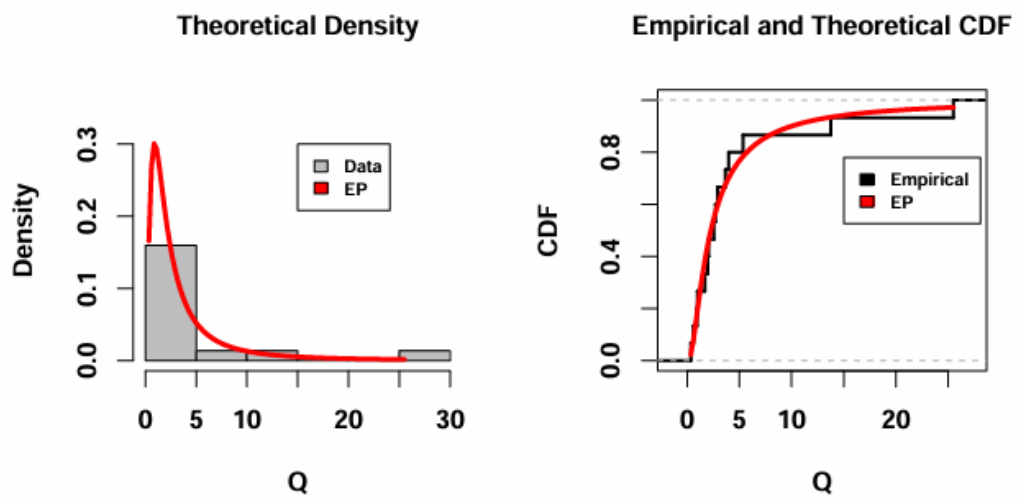

Figure 12. Estimated PDF and CDF for the second dataset.

In the previous sections, it was assumed that the estimates of ζ were analyzed after the stress, and strength random variables were assumed to follow the EPD with the same shape parameter ρ. Therefore, we also need to check if the parameters of their second shape are the same to estimate it using actual data.

First, it is assumed that $V \sim EPD\ (\mu_1, \rho_1)$ and $Q \sim EPD\ (\mu_2, \rho_2)$. We perform the following testing of hypothesis; $H_0 : \rho_1 = \rho_2$ *vs* $H_1 : \rho_1 \neq \rho_2$. The MLEs of $\mu_1, \rho_1, \mu_2,$ and ρ_2 are as follows: $\mu_{1(MLE)} = 1.4873, \hat{\rho}_{1(MLE)} = 0.4894, \hat{\mu}_{2(MLE)} = 3.7102, \hat{\rho}_{2(MLE)} = 1.4930$ and the log-likelihood value is $\log L_1 = -103.2001$.

Second, suppose that $V \sim EPD\ (\mu_1, \rho)$ and $Q \sim EPD\ (\mu_2, \rho)$, the MLEs of $\mu_1, \mu_2,$ and ρ are as follows: $\hat{\mu}_{1(MLE)} = 2.0445, \hat{\mu}_{2(MLE)} = 1.5645, \hat{\rho}_{(MLE)} = 0.7117,$ and the log-likelihood value is $\log L_2 = -106.8923$. Then the likelihood ratio statistic is constructed as follows:

$$LR = -2\log\left(\frac{L_2(\mu_1,\mu_2,\rho)}{L_1(\mu_1,\rho_1,\mu_2,\rho_2)}\right) = -2\ \left(\log L_2\ -\ \log L_1\right)\ = 7.3843.$$

Hence, the null hypothesis cannot be rejected. Therefore, in this case, the assumption of $\rho_1 = \rho_2$ is justified. Thus, both tests accept the null hypothesis that each dataset is drawn from EPD.

Following the above-described process, the MLEs, BEs, and the BCIs of the 95% of boot-p and boot-t are obtained in Table 3. Under SELF, WSELF, and MLF, the BEs are acquired along with their HPD interval. Since we do not know anything about the parameter beforehand, we presume that the hyper-parameter values are $\alpha_1 = \alpha_2 = \alpha_3 = \beta_1 = \beta_2 = \beta_3 = 0.0001$. The results in Table 3 show that posterior standard deviation (PSD) of the BEs is lower than that of the other MLEs. The findings indicate that the EPD parameters' BE is the most accurate. Interestingly, compared to the ML approach, the Bayesian methodology is more reliable.

Table 3. The MLEs, Bootstrap CIs, BEs of ζ, and their SEs, PSD, BCI, and HPD intervals

MLE		Boot-t	Boot-p	NIP							
		AIL	AIL	SELF		WSELF		MLF		AIL	CP
$\hat{\zeta}_{MLE}$	$\hat{\zeta}_{SE}$			$\tilde{\zeta}_{SELF}$	$\tilde{\zeta}_{SELF\_PSD}$	$\tilde{\zeta}_{WSELF}$	$\tilde{\zeta}_{WSELF\_PSD}$	$\tilde{\zeta}_{MLF}$	$\tilde{\zeta}_{MLF\_PSD}$		
0.2343	0.0157	0.7479	0.2567	0.3016	0.00516	0.2412	0.0087	0.1728	0.0076	0.4740	95.0125

Overall, analysis of the electrical insulation datasets supports the use of the EPD as a suitable model, considering the data's skewness and heavy tails. In relation to SSM, the reliability can be understood as the probability of the fact that the electrical insulation stress value in one period does not exceed the strength in another period. From the results of the study, it follows that BEs show better stability and reliability compared to MLEs, especially when estimating intervals. Additionally, HPD intervals prove to be shorter than other intervals.

Figure 13 displays the diagnostic plots for SSM. After the burn-in time, the trace plot displays strong mixing, and the cumulative mean stabilizes, suggesting convergence. The posterior distribution seems to be left-skewed and unimodal. The analysis's credibility is further increased by the decreasing autocorrelation, which suggests that the samples get increasingly independent over time. The MCMC chain seems to be dependable overall for posterior inference and estimation.

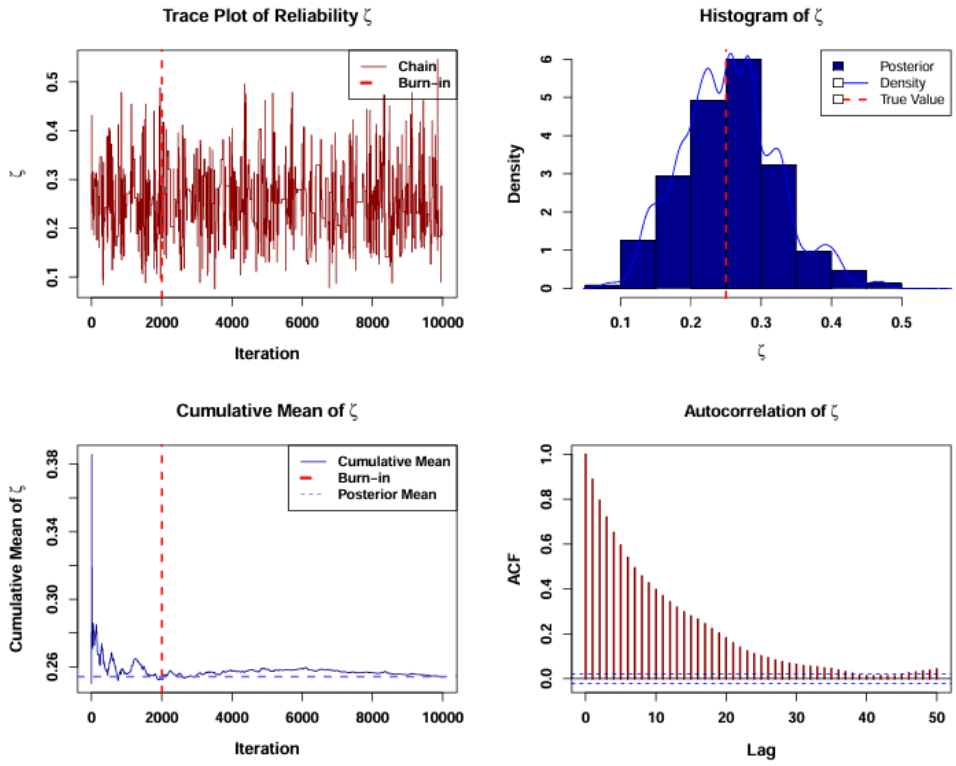

Figure 13. The MCMC diagnostic plots of ζ for the first real datasets.

7. Conclusions

In certain real-world scenarios, time and sample size constraints will prevent a researcher from accessing all the data. Consequently, this requires the creation of reliable estimation techniques based on the data at hand, especially those that use suitable sampling approaches to increase estimator efficiency. The SSM $\zeta = Pr\,(Q < V)$ is estimated in this work using LRRSS. The EPD with a common second shape parameter is followed by the stress and strength variables. For estimation, the maximum likelihood and Bayesian estimators under different loss functions (SELF, WSELF, and MLF) are obtained. The BCIs are constructed using the MCMC approach, and two parametric bootstrap methods are developed. A thorough Monte Carlo simulation study is created to assess the accuracy of estimators. According to a simulation study, the BEs computed under loss functions outperform a comparable MLE. In general, the BEs obtained under MLF perform better than those listed under SELF and WSELF. However, those under SELF yield the worst results when compared to other BEs. The BCIs perform better than boot-p and boot-t intervals for IPs and NIPs. It is shown that the boot-p CIs estimates are superior, yielding higher CP and narrower AIL compared to the boot-t CIs estimates.

The methodology's efficacy and utility are further supported by two real datasets from physical science applications. Among all estimation methods under consideration, the Bayesian approach under the MLF is recommended as a preferred method for these electrical insulation datasets, as it has the smallest SE, which is consistent with the simulation results in Section 5. Finally, LRRSS gathers data that are more instructive about the lower tail of the population, where failure or stress-strength events are most likely to occur, in contrast to simple random sampling or regular record sampling. Each record's effective information content is raised by this focused selection, which reduces sampling variability and produces more reliable parameter estimates. This feature of LRRSS results in notably smaller MSEs and more constrained BCIs in our simulation findings. Furthermore,

LRRSS saves money and time while maintaining high estimation efficiency since it effectively employs partial ranking as opposed to a full assessment. Therefore, a theoretically sound and empirically proven paradigm for stress-strength reliability analysis is provided by combining the EPD, which can simulate heavy tails, with the LRRSS, which is focused on lower-tail efficiency.

Nonetheless, there are some limitations to this study. First, there is an assumption that stress and strength would share a similar shape parameter ρ. Second, it is difficult to implement LRRSS in practice due to the need to continuously monitor the selection of smaller record units. Last, the performance of the suggested estimators needs to be tested using actual reliability data rather than the selected real data.

Researchers can expand on this work in various ways. To enable more flexible modeling of asymmetric reliability structures, the model could be expanded to include separate shape parameters for the stress and strength variables. Examining how well the suggested estimators work under progressive or hybrid sampling schemes is another crucial avenue that could lead to more adaptable data collection techniques in real-world applications. Additionally, adding hierarchical or adaptive Bayesian priors may improve the resilience of the model, particularly in situations with censored or small samples. Last, empirical research on actual engineering reliability data would support the LRRSS of EPD under SSM framework's practical applicability and point out possible changes for field deployment.

Author contributions

Amal S. Hassan: Conceptualization, methodology, investigation, editing, writing-original and review draft; Mohamed A. Abd Elgawad: Conceptualization, methodology, investigation, editing, writing-review; Majdah Mohammed Badr: Conceptualization, investigation, editing, writing-review; Rokaya Elmorsy Mohamed: Conceptualization, methodology, writing-original and review draft, investigation, editing, software. All authors have read and approved the final manuscript.

Use of Generative-AI tools declaration

The authors declare that the use of AI tools is limited to language editing. All scientific content, proofs, results, and conclusions were developed and independently verified by the authors.

Funding

This work was supported and funded by the Deanship of Scientific Research at Imam Mohammad Ibn Saud Islamic University (IMSIU) (grant number IMSIU-DDRSP2601).

Acknowledgments

The authors would like to express their thanks to the editor and the five anonymous referees for valuable comments and helpful observations. Imam Mohammad Ibn Saud Islamic University Researchers Supporting Project number (IMSIU-DDRSP2601), Imam Mohammad Ibn Saud Islamic University, Riyadh, Saudi Arabia.

Conflict of interest

The authors declare no conflict of interest.

Appendix

Table A.1. ABs and MSEs for EPD for MLEs and IP and NIP.

m_1	m_2	MLE		IP						NIP					
				SELF		WSELF		MLF		SELF		WSELF		MLF	
		AB	MSE	AB	MSE	AB	MSE	AB	MSE	AB	MSE	AB	MSE	AB	MSE
$\zeta = 0.25$															
3	3	0.09582	0.01368	0.08311	0.00691	0.07038	0.00495	0.05697	0.00325	0.09325	0.01176	0.09251	0.01057	0.09085	0.00977
	5	0.09110	0.01201	0.05777	0.00334	0.06418	0.00412	0.07075	0.00501	0.06331	0.00401	0.07113	0.00506	0.07921	0.00627
	7	0.08898	0.01072	0.05933	0.00352	0.06465	0.00418	0.06990	0.00489	0.05928	0.00351	0.06698	0.00449	0.07422	0.00551
5	3	0.08572	0.01151	0.09271	0.00860	0.08030	0.00645	0.06821	0.00465	0.13413	0.01799	0.11706	0.01370	0.10003	0.01001
	5	0.07886	0.00936	0.04728	0.00224	0.05307	0.00282	0.05887	0.00147	0.05540	0.00307	0.06292	0.00296	0.07053	0.00197
	7	0.07479	0.00767	0.04995	0.00250	0.05495	0.00302	0.05986	0.00358	0.05144	0.00265	0.05687	0.00323	0.06254	0.00391
7	3	0.07650	0.00977	0.07281	0.00530	0.06429	0.00413	0.05577	0.00311	0.11931	0.01423	0.10203	0.01041	0.08500	0.00722
	5	0.07094	0.00805	0.03935	0.00155	0.04459	0.00199	0.04974	0.00247	0.06180	0.00382	0.06993	0.00489	0.07777	0.00605
	7	0.05908	0.00606	0.04196	0.00176	0.04626	0.00214	0.05057	0.00106	0.06138	0.00377	0.06810	0.00204	0.07467	0.00158
$\zeta = 0.50$															
3	3	0.12539	0.02349	0.07967	0.00635	0.07133	0.00509	0.06246	0.00390	0.14413	0.02077	0.13445	0.01808	0.12394	0.01536
	5	0.11832	0.02129	0.07770	0.00604	0.08464	0.00716	0.09180	0.00843	0.09560	0.00914	0.10492	0.01101	0.11481	0.01318
	7	0.11824	0.02151	0.07795	0.00608	0.08371	0.00701	0.08954	0.00802	0.09003	0.00811	0.09874	0.00975	0.10734	0.01152
5	3	0.10832	0.01813	0.09109	0.00830	0.08492	0.00721	0.07876	0.00620	0.14437	0.02084	0.13466	0.01813	0.12453	0.01551
	5	0.09846	0.01486	0.06018	0.00362	0.05568	0.00331	0.07123	0.00237	0.08276	0.00985	0.09135	0.00835	0.10033	0.00701
	7	0.09374	0.01335	0.06468	0.00418	0.06987	0.00488	0.07524	0.00566	0.07624	0.00581	0.08237	0.00678	0.08884	0.00789
7	3	0.10421	0.01654	0.10013	0.01003	0.09461	0.00895	0.08898	0.00792	0.12962	0.01680	0.11935	0.01424	0.10866	0.01181
	5	0.09484	0.01336	0.04821	0.00232	0.05315	0.00282	0.05808	0.00337	0.09375	0.00879	0.10323	0.01066	0.11276	0.01272
	7	0.07343	0.00836	0.05160	0.00266	0.05671	0.00202	0.06188	0.00183	0.09264	0.00808	0.10046	0.00601	0.10838	0.00517
$\zeta = 0.95$															
3	3	0.04728	0.00618	0.02297	0.00053	0.02258	0.00051	0.02218	0.00049	0.02539	0.00064	0.02503	0.00063	0.02467	0.00061
	5	0.04773	0.00650	0.02032	0.00041	0.02066	0.00043	0.02100	0.00044	0.02321	0.00054	0.02357	0.00056	0.02394	0.00057
	7	0.05111	0.00750	0.01956	0.00038	0.01987	0.00039	0.02018	0.00041	0.02367	0.00056	0.02396	0.00057	0.02425	0.00059
5	3	0.03579	0.00272	0.02111	0.00045	0.02088	0.00044	0.02066	0.00043	0.02487	0.00062	0.02462	0.00061	0.02437	0.00059
	5	0.03811	0.00377	0.01688	0.00028	0.01711	0.00026	0.01735	0.00020	0.02051	0.00042	0.02081	0.00040	0.02110	0.00035
	7	0.03899	0.00396	0.01234	0.00015	0.01255	0.00016	0.01275	0.00016	0.01843	0.00034	0.01863	0.00035	0.01883	0.00035
7	3	0.04051	0.00383	0.01720	0.00030	0.01685	0.00028	0.01650	0.00027	0.02396	0.00057	0.02359	0.00056	0.02321	0.00054
	5	0.04223	0.00482	0.01850	0.00034	0.01877	0.00035	0.01904	0.00036	0.02398	0.00057	0.02432	0.00059	0.02466	0.00061
	7	0.03564	0.00329	0.01226	0.00020	0.01250	0.00016	0.01275	0.00012	0.01377	0.00036	0.01405	0.00033	0.01433	0.00039

Table A.2. AIL and CP (in %) for EPD for BCIs and BEs.

m_1	m_2	Boot-t		Boot-p		IP		NIP	
		AIL	CP	AIL	CP	AIL	CP	AIL	CP
$\zeta = 0.25$									
	3	0.95392	92.1	0.89217	94.7	0.23381	96.1	0.29641	95.9
3	5	0.37385	93.3	0.60127	95.2	0.13062	96.8	0.14217	96.4
	7	0.40357	94.0	0.42067	95.5	0.11776	97.3	0.13485	95.5
	3	0.92584	93.5	0.64030	95.0	0.24996	97.4	0.29700	96.4
5	5	0.44566	94.2	0.33354	95.7	0.12536	97.4	0.13767	96.4
	7	0.39099	94.8	0.28235	95.8	0.11879	96.8	0.12417	97.0
	3	0.65731	93.9	0.57787	95.3	0.19100	96.8	0.29484	95.6
7	5	0.34020	94.6	0.32970	95.9	0.11860	97.4	0.14615	97.8
	7	0.38808	95.0	0.24962	96.0	0.11120	97.8	0.12818	97.3
$\zeta = 0.50$									
	3	0.89474	91.8	0.81110	94.5	0.24608	96.5	0.28614	96.1
3	5	0.82037	93.0	0.77996	95.3	0.19484	97.1	0.22455	95.1
	7	0.62814	94.1	0.76046	95.7	0.18472	97.0	0.20461	95.5
	3	0.90342	93.2	0.79459	95.1	0.22722	96.6	0.28499	95.1
5	5	0.58667	94.4	0.55822	95.8	0.18169	96.3	0.21497	96.0
	7	0.66040	94.9	0.54496	96.0	0.17948	96.1	0.18861	95.9
	3	0.69686	93.8	0.66678	95.4	0.20754	96.4	0.29428	95.6
7	5	0.53615	94.7	0.58297	96.0	0.16552	97.0	0.22410	96.4
	7	0.36242	95.1	0.33746	96.2	0.17487	96.9	0.20282	96.8
$\zeta = 0.95$									
	3	0.97832	88.5	0.83527	94.3	0.05958	97.1	0.05499	96.9
3	5	0.11631	89.7	0.13552	94.7	0.05918	98.6	0.06560	98.3
	7	0.14195	90.9	0.28183	95.0	0.06077	97.9	0.05702	96.6
	3	0.86548	90.2	0.74193	94.6	0.05015	98.5	0.04907	97.9
5	5	0.10717	91.5	0.13781	95.1	0.05675	98.6	0.05785	98.3
	7	0.11193	92.3	0.17328	95.4	0.05163	98.8	0.04775	98.6
	3	0.78832	91.0	0.73151	94.9	0.06275	98.4	0.05939	97.8
7	5	0.10124	92.2	0.13166	95.3	0.05500	98.5	0.06116	97.9
	7	0.11420	93.1	0.15122	95.5	0.05615	99.3	0.05947	99.1

References

1. K. Chandler, The distribution and frequency of record values, *J. Roy. Statist. Soc. B*, **14** (1952), 220–228. https://doi.org/10.1111/j.2517-6161.1952.tb00115.x
2. F. Foster, A. Stuart, Distribution-free tests in time-series based on the breaking of records, *J. Roy. Statist. Soc. B*, **16** (1954), 1–22. https://doi.org/10.1111/j.2517-6161.1954.tb00143.x
3. G. A. McIntyre, A method for unbiased selective sampling using ranked set, *Am. Stat.*, **59** (2005), 230–232. https://doi.org/10.1198/000313005X54180
4. K. Takahasi, K. Wakimoto, On unbiased estimates of the population mean based on the sample stratified by means of ordering, *Ann. I. Stat. Math.*, **20** (1968), 1–31. https://doi.org/10.1007/BF02911622
5. M. Chen, W. Chen, C. Deng, Some new results on parameter estimation of the exponential-Poisson distribution in ranked set sampling, *Appl. Math. Ser. B*, **40** (2025), 413–428. https://doi.org/10.1007/s11766-025-4927-4
6. M. Chen, W. Chen, R. Yang, Double moving extremes ranked set sampling design, *Acta Math. Appl. Sin.-E.*, **40** (2024), 75–90. https://doi.org/10.1007/s10255-024-1104-9
7. R. Yang, W. Chen, M. Chen, Y. Zhou, Maximum likelihood estimation of the parameters of the inverse Gaussian distribution using maximum ranked set sampling with unequal samples, *Math. Popul. Stud.*, **30** (2023), 1–21. https://doi.org/10.1080/08898480.2021.1996822
8. M. Salehi, J. Ahmadi, Record ranked set sampling scheme, *Metron*, **72** (2014), 351–365. https://doi.org/10.1007/s40300-014-0038-z
9. C. Arnold, N. Balakrishnan, H. N. Nagaraja, *Records*, New York: Wiley, 1998. https://doi.org/10.1002/9781118150412
10. M. Salehi, J. Ahmadi, S. Dey, Comparison of two sampling schemes for generating record breaking data from the proportional hazard rate models, *Commun. Stat.-Theory M.*, **45** (2016), 3721–3733. https://doi.org/10.1080/03610926.2014.909938
11. M. Eskandarzadeh, S. Tahmasebi, M. Afshari, Information measures for record ranked set samples, *Cienc. Nat.*, **38** (2016), 554–563. https://doi.org/10.5902/2179460X19527
12. J. Paul, P. Y. Thomas, Concomitant record ranked set sampling, *Commun. Statist. Theory Methods*, **46** (2017), 9518–9540. https://doi.org/10.1080/03610926.2016.1213286
13. A. Safarian, M. Arashi, R. A. Belaghi, Improved estimators for stress–strength reliability using record ranked set sampling scheme, *Commun. Stat.-Simul. C.*, **48** (2019), 2708–2726. https://doi.org/10.1080/03610918.2018.1468451
14. A. Sadeghpour, M. Salehi, A. Nezakati, Estimation of the stress–strength reliability using lower record ranked set sampling scheme under the generalized exponential distribution, *J. Stat. Comput. Sim.*, **90** (2020), 51–74. https://doi.org/10.1080/00949655.2019.1672694
15. Y. Dong, W. Gui, Reliability estimation in stress–strength for generalized Rayleigh distribution using a lower record ranked set sampling scheme, *Mathematics*, **12** (2024), 1650. https://doi.org/10.3390/math12111650
16. Z. W. Birnbaum, On a use of Mann–Whitney statistics, *P. Third Berkeley Symp. Math. Stat. Probab.*, **1** (1956), 13–17. https://doi.org/10.1525/9780520313880-005
17. S. Kotz, Y. Lumelskii, M. Pensky, *The stress–strength model and its generalizations: Theory and applications*, Singapore: World Scientific, 2003. https://doi.org/10.1142/9789812564511
18. D. Kundu, R. D. Gupta, Estimation of P(X<Y) for generalized exponential distribution, *Metrika*, **61** (2005), 291–308. https://doi.org/10.1007/s001840400345

19. M. Z. Raqab, T. Madi, D. Kundu, Estimation of P(Y<X) for the three-parameter generalized exponential distribution, *Commun. Stat.-Theory M.*, **37** (2008), 2854–2865. https://doi.org/10.1080/03610920802162664
20. C. Kim, Y. Chung, Bayesian estimation of P(Y<X) from Burr type X model containing spurious observations, *Stat. Pap.*, **47** (2006), 643–656. https://doi.org/10.1007/s00362-006-0310-2
21. A. S. Hassan, A. M. A. Elghaffar, E-Bayesian and hierarchical Bayesian stress–strength reliability modeling under partially accelerated life testing, *J. Stat. Theory Pract.*, **20** (2026), 21. https://doi.org/10.1007/s42519-025-00532-5
22. E. A. Ahmed, L. A. Al-Essa, Inference of stress–strength reliability based on adaptive progressive type-II censoring from Chen distribution with application to carbon fiber data, *AIMS Math.*, **9** (2024), 20482–20515. https://doi.org/10.3934/math.2024996
23. A. K. Mahto, K. Abhishek, Y. M. Tripathi, O. S. Balogun, Y. A. Tashkandy, M. E. Bakr, On multicomponent stress–strength reliability for progressively censored logistic exponential model, *Alex. Eng. J.*, **127** (2025), 830–847. https://doi.org/10.1016/j.aej.2025.06.004
24. H. A. Newer, Multicomponent stress–strength reliability analysis using the inverted exponentiated Rayleigh distribution under block adaptive type-II progressive hybrid censoring and k-records, *Sci. Rep.*, **15** (2025), 43820. https://doi.org/10.1038/s41598-025-30570-9
25. S. G. Nassr, O. Abo-Kasem, R. H. Khashab, E. Alshawarbeh, S. S. Alshqaq, N. M. Elharoun, Reliability analysis of inverted exponentiated Rayleigh parameters via progressive hybrid censoring data with applications in medical data, *PLoS One*, **20** (2025), e0336169. https://doi.org/10.1371/journal.pone.0336169
26. D. Abdo, A. A. El-Saeed, A. Abdelmegaly, Evaluating fit of some survival analysis models with application and simulation, *Egypt. Stat. J.*, **68** (2024), 86–103. https://doi.org/10.21608/esju.2024.314785.1040
27. A. S. Hassan, A. M. A. Elghaffar, Inference on stress–strength reliability model under step-stress partially accelerated life testing based on the Lomax distribution, *Qual. Quant.*, 2026. https://doi.org/10.1007/s11135-026-02648-7
28. T. Erbayram, Y. Akdoğan, C. Chesneau, Stress–strength reliability for the Poisson–Lindley distribution based on the ranked set sample method, *B. Iran. Math. Soc.*, **51** (2025), 52. https://doi.org/10.1007/s41980-025-00980-6
29. A. Baklizi, Estimation of P(X<Y) using record values in the one and two parameter exponential distributions, *Commun. Stat.-Theor. M.*, **37** (2008), 692–698. https://doi.org/10.1080/03610920701501921
30. M. Basirat, S. Baratpour, J. Ahmadi, On estimation of stress–strength parameter using record values from proportional hazard rate models, *Commun. Stat.-Theor. M.*, **45** (2016), 5787–5801. https://doi.org/10.1080/03610926.2014.948727
31. F. Condino, F. Domma, G. Latorre, Likelihood and Bayesian estimation of P(Y<X) using lower record values from a proportional reversed hazard family, *Stat. Pap.*, **59** (2018), 467–485. https://doi.org/10.1007/s00362-016-0772-9
32. R. M. Juvairiyya, P. Anilkumar, Estimation of stress–strength reliability for the Pareto distribution based on upper record values, *Statistica*, **78** (2018), 397–409. https://doi.org/10.6092/issn.1973-2201/8242
33. A. Chaturvedi, A. Malhotra, On estimation of stress–strength reliability using lower record values from proportional reversed hazard family, *Am. J. Math. Manag. Sci.*, **39** (2020), 234–251. https://doi.org/10.1080/01966324.2020.1722299

34. A. Pak, M. Z. Raqab, M. R. Mahmoudi, S. S. Band, A. Mosavi, Estimation of stress–strength reliability R=P(X>Y) based on Weibull record data in the presence of inter-record times, *Alex. Eng. J.*, **61** (2022), 2130–2144. https://doi.org/10.1016/j.aej.2021.07.025
35. Y. Yu, L. Wang, S. Dey, J. Liu, Estimation of stress–strength reliability from unit-Burr III distribution under records data, *Math. Biosci. Eng.*, **20** (2023), 12360–12379. https://doi.org/10.3934/mbe.2023550
36. B. Elkalzah, M. O. Mohamed, K. Elsharkawy, E. S. Osman, A. Aldukeel, G. A. Marei, Classical and Bayesian estimation of stress–strength reliability under the discrete alpha-power Weibull distribution with incomplete and record data: Application to high-voltage capacitors, *AIMS Math.*, **11** (2026), 6374–6399. https://doi.org/10.3934/math.2026263
37. A. S. Hassan, T. Alballa, E. Alshawarbeh, D. Basalamah, S. G. Nassr, R. E. Mohamed, Reliability analysis in stress–strength model under record values with practical verification, *Sci. Rep.*, 2026. https://doi.org/10.1038/s41598-026-39638-6
38. J. Pickands, Statistical inference using extreme order statistics, *Ann. Stat.*, **3** (1975), 119–131. https://doi.org/10.1214/aos/1176343003
39. J. Chen, C. Cheng, Reliability of stress–strength model for exponentiated Pareto distributions, *J. Stat. Comput. Sim.*, **87** (2017), 791–805. https://doi.org/10.1080/00949655.2016.1226309
40. R. Gupta, R. D. Gupta, P. L. Gupta, Modeling failure time data by Lehmann alternatives, *Commun. Stat.-Theor. M.*, **27** (1998), 887–904. https://doi.org/10.1080/03610929808832134
41. K. Aarssen, L. de Haan, On the maximal life span of humans, *Math. Popul. Stud.*, **4** (1994), 259–281. https://doi.org/10.1080/08898489409525379
42. G. R. Daragahi-Noubary, On tail estimation: an improved method, *Math. Geol.*, **21** (1989), 829–842. https://doi.org/10.1007/BF00894450
43. D. Zelterman, A statistical distribution with an unbounded hazard function and its application to a theory from demography, *Biometrics*, **48** (1992), 807–818. https://doi.org/10.2307/2532346
44. N. Mole, C. W. Anderson, S. Nadarajah, C. Wright, A generalised Pareto distribution model for high concentrations in short-range atmospheric dispersion, *Environmetrics*, **6** (1995), 595–606. https://doi.org/10.1002/env.3170060606
45. A. S. Hassan, Y. S. Morgan, Bayesian and frequentist analysis of stress–strength reliability modeling involving outliers with application to insurance data, *J. Inf. Data Manag.*, 2026. https://doi.org/10.1007/s42488-025-00158-z
46. S. Saini, Advancements in reliability estimation for the exponentiated Pareto distribution: A comparison of classical and Bayesian methods with lower record values, *Computation Stat.*, **40** (2025), 353–382. https://doi.org/10.1007/s00180-024-01497-y
47. F. G. Akgül, Classical and Bayesian estimation of multicomponent stress–strength reliability for exponentiated Pareto distribution, *Soft Comput.*, **25** (2021), 9185–9197. https://doi.org/10.1007/s00500-021-05902-2
48. E. M. Almetwally, A. S. Hassan, Enhanced estimators for the multi-stress strength reliability using an advanced progressive hybrid censoring scheme, *AIMS Math.*, **11** (2026), 7740–7765. https://doi.org/10.3934/math.2026318
49. M. J. Nooghabi, On estimation in the exponentiated Pareto distribution in the presence of outliers, *Appl. Math. Inform. Sci.*, **11** (2017), 1129–1137. https://doi.org/10.18576/amis/110420
50. M. A. E. Mahmoud, N. M. Yhiea, S. M. El-Said, Estimation of parameters for the exponentiated Pareto distribution based on progressively type-II right censored data, *J. Egypt. Math. Soc.*, **24** (2016), 431–436. https://doi.org/10.1016/j.joems.2015.09.002

51. H. J. Khamnei, I. M. Kavaliauskiene, M. Fathi, A. Valackiene, S. Ghorbani, Parameter estimation of the exponentiated Pareto distribution using ranked set sampling and simple random sampling, *Axioms*, **11** (2022), 293. https://doi.org/10.3390/axioms11060293
52. R. J. Tibshirani, B. Efron, An introduction to the bootstrap, *Monogr. Stat. Appl. Probab.*, **57** (1993), 1–436. https://doi.org/10.1007/978-1-4899-4541-9_1
53. S. Dey, T. Dey, D. J. Luckett, Statistical inference for the generalized inverted exponential distribution based on upper record values, *Math. Comput. Simulat.*, **120** (2016), 64–78. https://doi.org/10.1016/j.matcom.2015.06.012
54. S. Singh, Y. M. Tripathi, Estimating the parameters of an inverse Weibull distribution under progressive type-I interval censoring, *Stat. Pap.*, **59** (2018), 21–56. https://doi.org/10.1007/s00362-016-0750-2
55. W. Nelson, Graphical analysis of accelerated life test data with the inverse power law model, *IEEE T. Reliab.*, **21** (1972), 2–11. https://doi.org/10.1109/TR.1972.5216164
56. J. F. Lawless, *Statistical models and methods for lifetime data*, 2 Eds., Hoboken, New Jersey: John Wiley & Sons, 2003. https://doi.org/10.1002/9781118033005

AIMS Press